PAPER REF: 3951

# A 3D VIBROACOUSTIC MODEL FOR THE PREDICTION OF UNDERWATER NOISE FROM OFFSHORE PILE DRIVING

**Apostolos Tsouvalas(*) and Andrei Metrikine**

Section of Structural Mechanics, Faculty of Civil Engineering and Geosciences , Delft University of Technology, The Netherlands

(*)*Email:* a.tsouvalas@tudelft.nl

## ABSTRACT

Steel monopiles are the most widely used foundation method of offshore wind turbines and are driven into place with the help of large hydraulic hammers. The installation process is accompanied with very high sound pressures at the surrounding water which are known to produce deleterious effects on both mammals and fish. In this work, a linear semi-analytical formulation of the coupled vibro-acoustics of a complete pile-fluid-soil interaction model is addressed. The pile is described by a thin shell theory whereas both fluid and soil are modelled as three-dimensional continua. It is shown that the near-field response in the fluid is dominated by pressure *Mach cones* due to the supersonic compressional waves in the pile generated by the impact hammer. The soil response is dominated by shear waves with almost vertical polarization. *Scholte* waves are generated at the soil-fluid interface which propagate with a velocity slightly lower than that of the shear waves in the soil. Their energy is mainly localized in a restricted zone close to the interface and therefore they experience much less attenuation in comparison to the other surface modes. A number of cases for which experimental data are available for comparison is analysed in order to show the ability of the model to provide reliable predictions and to highlight the strong and weak points of the model.

***Keywords:*** pile driving, vibro-acoustics, underwater acoustics, solid-fluid interaction, *Scholte* waves

## INTRODUCTION

The semi-analytical description introduced here is a follow-up work of a previous model developed by the same authors (A.Tsouvalas and A.V.Metrikine, 2013), but accounts additionally for a complete three dimensional description of the soil. The pile is described by an appropriate thin shell theory which includes the effects of both shear deformation and rotational inertia. The fluid is treated as a three-dimensional compressible medium with a pressure release boundary describing the sea surface. The soil is described as a three-dimensional continuum able to support both dilatational and shear waves and is terminated at the pile tip level with a rigid boundary. The influence of the rigid boundary is expected to be small for large penetration depths of the pile into the soil (H.R. Masoumi, G. Degrande, 2008). The solution of the system of coupled partial differential equations is based on the dynamic sub-structuring technique. The total system is divided into two sub-systems: the shell structure and the soil-fluid exterior. The linearity of the model allows for the representation of the response of each domain in the form of a superposition over appropriate eigenfunctions. It is shown that the set of eigenfunctions of each domain form a complete and orthogonal basis which allows for a suitable representation of the response of the coupled system. By enforcing force equilibrium and displacement compatibility at the interface between the shell structure and the exterior layered medium, the original system of coupled partial differential equations is reduced to a system of coupled algebraic equations which can be solved with high accuracy. This paper is structured as follows. At first, the mathematical model is described and a method is presented for obtaining the solution of the coupled system. Subsequently, a discussion takes place on the completeness of the modal sum and of the approximations inherently involved in such a representation. To examine the completeness of the modal sum, a solution based on the wavenumber integration technique is discussed and the results are compared with those ones obtained with the application of the separation of variables method. The equivalence of the two approaches of the problem analysed here is demonstrated. Finally, results are presented for a real case scenario and the influence of the soil properties on the vibro-acoustics of the system is thoroughly analysed.

## MODEL AND GOVERNING EQUATIONS

The geometry of the model is shown in Fig. 1. The shell is of finite length and occupies the domain $0 \le z \le L$. The constants $E$, $v$, $R$, $\rho$ and $2h$ correspond to the complex modulus of elasticity in the frequency domain, the Poisson ratio, the radius of the middle surface, the density and the thickness of the shell respectively. The soil occupies the region $z_2 \le z \le L$ for $r > R$. The interface at $z = L$ is substituted by a rigid boundary and the soil above it can consist of a number of layers with varying properties, all of them horizontally stratified. The soil material shows viscoelastic behaviour and the material damping is incorporated in the form of complex constants instead of the classical *Lamè* constants. The constants $\lambda_s$ and $\mu_s$ define the complex *Lamè* coefficients of the soil material and $v_s$ is the Poisson ratio that is assumed real valued. The fluid occupies the domain $z_1 \le z \le z_2$ for $r > R$ and is modelled with the linearised and compressible description. A small attenuation coefficient can be incorporated in the form of a complex wave speed.

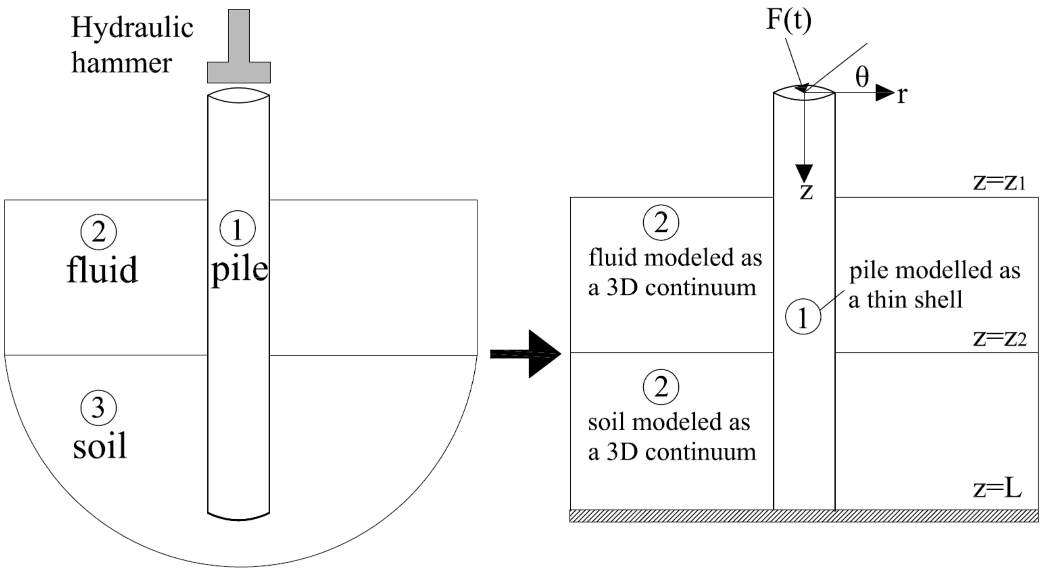


Fig.1 Geometry of the model and coordinate system definition

**Governing equations of the coupled system**

The system of equations is analytically derived here for the axially symmetric case in which the external force is applied at the pile head vertically. The equations of motion describing the vibro-acoustics of the coupled system read:

$$\{\mathbf{L}\}\ \mathbf{u}(z,t)+\{\mathbf{I}_{\mathbf{mod}}\}\ \mathbf{u}(z,t)=-\boldsymbol{\sigma}_s(R,z,t)\cdot H(z-z_2)+\mathbf{p}_f(R,z,t)\cdot[H(z-z_1)-H(z-z_2)]+\mathbf{F}_{ext}(z,t) \qquad (1)$$

In the equation above, $\mathbf{u}(z,t)$ is the displacement vector of the mid-surface of the shell. The terms $\{\mathbf{L}\}$ and $\{\mathbf{I}_{\mathbf{mod}}\}$ are the stiffness and modified inertia matrix operators of the shell respectively based on the applied thin shell theory. Their components are given in (A.Tsouvalas and A.V.Metrikine, 2013). The term $\boldsymbol{\sigma}_s(R,z,t)$ represents the boundary traction vector that takes into account the reaction of the soil surrounding the shell at $z_2 \le z \le L$. The term $\mathbf{p}_f(R,z,t)$ represents the fluid pressure exerted at the outer surface of the shell at $z_1 \le z \le z_2$. The functions $H(z-z_i)$ are the Heaviside step functions which are used here to account for the fact that the soil and the fluid are in contact with different segments of the shell. For the cylindrically symmetric case discussed in this section the angular dependence drops from all terms in Eq.(1).

The motion of the fluid is fully characterized by a scalar velocity potential $\varphi_e(r,z,t)$. The equation of motion for the outer fluid domain reads:

$$\nabla^2\varphi_f(r,z,t)-\frac{1}{c_f^2}\varphi_f(r,z,t)=0 \qquad (2)$$

, where $c_f$ is the sound speed in the exterior fluid domain and the *Laplacian* operator $\nabla^2$ is defined in the cylindrical coordinate system. The pressure in the fluid and the velocity vector are given by:

$$p_f(r,z,t)=-\rho_{f,2}\cdot\frac{\partial\varphi(r,z,t)}{\partial t} \qquad (3)$$

$\mathbf{v}_f(r,z,t)=\boldsymbol{\nabla}\varphi_f(r,z,t)$, with $\nabla$ being the well-known *Nabla* operator. (4)

The motion of the soil medium is described by the following set of linear equations:

$$\mu\cdot\boldsymbol{\nabla}^2\mathbf{u}+(\lambda_s+\mu_s)\cdot\boldsymbol{\nabla\nabla}\cdot\mathbf{u}=\rho_s\cdot\frac{\partial^2\mathbf{u}}{\partial t^2} \qquad (5)$$

The constitutive and geometrical relations for the soil medium read:

$$\sigma_{ij}=\lambda\cdot\varepsilon_{kk}\cdot\delta_{ij}+2\cdot\mu\cdot\varepsilon_{ij} \qquad (6)$$

$$\varepsilon_{ij}=\frac{1}{2}\cdot\left(u_{i,j}+u_{j,i}\right) \qquad (7)$$

The Helmholtz decomposition is applied, i.e. $\mathbf{u}=\boldsymbol{\nabla}\varphi_s+\boldsymbol{\nabla}\times\psi_s$, in which two scalar potentials are introduced for the axial symmetric case, which satisfy two uncoupled equations of motion:

$$\boldsymbol{\nabla}^2\varphi_s(r,z,t)-\frac{1}{c_L^2}\varphi_s(r,z,t)=0 \qquad (8)$$

$$\boldsymbol{\nabla}^2\psi_s(r,z,t)-\frac{1}{c_T^2}\psi_s(r,z,t)=0 \qquad (9)$$

, in which: $c_L = \sqrt{(\lambda_s + 2\mu_s)/\rho}$, $c_T = \sqrt{\mu_s/\rho}$ correspond to the phase velocity of the compressional and shear waves respectively. Since we work in the linear regime, the solution can be searched for in the frequency domain. The integral Fourier transform with respect to time of the aforementioned set of equations yields:

$$\{\mathbf{L}\}\,\tilde{\mathbf{u}}(z,\omega) + \{\tilde{\mathbf{I}}_{\mathbf{mod}}\}\,\tilde{\mathbf{u}}(z,\omega) = -\tilde{\boldsymbol{\sigma}}_s(R,z,\omega)\cdot H(z-z_2) + \tilde{\mathbf{p}}_f(R,z,\omega)\cdot[H(z-z_1) - H(z-z_2)] + \tilde{\mathbf{f}}_{ext}(z,\omega) \quad (10)$$

$$\nabla^2\tilde{\varphi}_f(r,z,\omega) + k_f^2\cdot\tilde{\varphi}_f(r,z,\omega) = 0 \quad (11)$$

$$\nabla^2\tilde{\varphi}_s(r,z,\omega) + k_L^2\cdot\tilde{\varphi}_s(r,z,\omega) = 0 \quad (12)$$

$$\nabla^2\tilde{\psi}_s(r,z,\omega) + k_T^2\cdot\tilde{\psi}_s(r,z,\omega) = 0 \quad (13)$$

, in which $k_f^2 = \dfrac{\omega^2}{c_f^2}$, $k_L^2 = \dfrac{\omega^2}{c_L^2}$ and $k_T^2 = \dfrac{\omega^2}{c_T^2}$. Eqs. (10) - (13) form the set of equations in the Fourier domain. The task is therefore reduced to the derivation of the complex amplitudes $\tilde{\varphi}_s(r,z,\omega)$, $\tilde{\varphi}_f(r,z,\omega)$ and $\tilde{\psi}_s(r,z,\omega)$ in the frequency domain. Once these are known the solution in the time domain can be found by using an inverse Fourier transform.

**Boundary and interface conditions**

In addition to the governing equations, the coupled system should satisfy a set of boundary and interface conditions. The boundary conditions along the vertical coordinate read:

- *Boundary condition at the fluid surface* ($z = z_1$):

$$\tilde{p}_f(r,z=z_1,\omega) = 0 \quad (14)$$

- *Interface condition at the seabed surface* ($z = z_2$):

$$\tilde{\sigma}_{zz}(r,z=z_2,\omega) + \tilde{p}_f(r,z=z_2,\omega) = 0 \quad (15)$$

$$\tilde{\sigma}_{zr}(r,z=z_2,\omega) = 0 \quad (16)$$

$$\tilde{u}_z(r,z=z_2,\omega) - \frac{1}{\mathrm{i}\cdot\omega}\cdot\tilde{v}_{z,f}(r,z=z_2,\omega) = 0 \quad (17)$$

- *Boundary condition at the soil bottom* ($z = L$):

$$\tilde{u}_z(r,z=L,\omega) = 0 \quad (18)$$

$$\tilde{u}_r(r,z=L,\omega) = 0 \quad (19)$$

The boundary conditions along the radial coordinate read:

- *Radiation condition at infinity ($r \to \infty$)*:

$$\lim_{r\to\infty} r\cdot\left(\frac{\partial\tilde{\varphi}_{f;s}}{\partial r} + k_{f;L}\cdot\tilde{\varphi}_{f;s}\right) = 0 \text{ and } \lim_{r\to\infty} r\cdot\left(\frac{\partial\tilde{\psi}_s}{\partial r} + k_T\cdot\tilde{\psi}_s\right) = 0 \quad (20)$$

- *Interface conditions along the shell-fluid and shell-soil interface ($r = R$):*

$$\tilde{u}_{r,shell}(z_1 \le z \le z_2,\omega) - \frac{1}{\mathrm{i}\cdot\omega}\cdot\tilde{v}_{r,f}(r=R, z_1 \le z \le z_2,\omega) = 0 \quad (21)$$

$$\tilde{u}_{r,shell}(z_2 \le z \le L,\omega) - \tilde{u}_{r,s}(r=R, z_2 \le z \le L,\omega) = 0 \quad (22)$$

$$\tilde{u}_{z,shell}(z_2 \le z \le L,\omega) - \tilde{u}_{z,s}(r=R, z_2 \le z \le L,\omega) = 0 \quad (23)$$

The set of equations (10)-(23) describes the coupled vibro-acoustics of the system in the frequency domain.

## SOLUTION TO THE COUPLED SYSTEM OF EQUATIONS

The response of the system is sought for in the form of a modal expansion with respect to the *in vacuo* shell modes and to the modes of the soil-fluid domain. The analytical approach is based on the following steps: **i)** solution of the eigenvalue problem of the shell without the presence of the fluids and the soil; **ii)** solution of the eigenvalue problem of the soil-fluid exterior domain; **iii)** solution of the coupled system of equations resulting from the substitution of the obtained solutions for the shell and the soil-fluid domain into the interface conditions.

### Eigen-vibrations of the shell structure

The procedure for calculating the eigenfrequencies and eigenmodes of a circular cylindrical shell with arbitrary edge constraints is standard and can be found, for example, in (A.Tsouvalas and A.V.Metrikine, 2013). The analytical solution is based on a coupled system of partial differential equations describing the free vibrations of the shell, i.e. homogeneous part of Eq.(1), which includes the effects of both shear deformation and rotational inertia. The final solution per vibration mode can be expressed in the following form:

$$u_{jnm}(z,t) = A_{nm} \cdot U_{jnm}(z) \cdot \exp\left(\mathrm{i}\ \Omega_{nm}\ \mathrm{t}\right), \text{ with } n = 0. \tag{24}$$

The index $j = r, z$ indicates the corresponding displacement component, $n = 0$ is the circumferential order (for the axially symmetric case) and $m = 1,2,...,\infty$ is the axial order. The functions $U_{z0m}(z)$ and $U_{r0m}(z)$ describe the axial distribution for the axial and radial displacement fields respectively; $\Omega_{0m}$ is the eigenfrequency. The unknown modal factors $A_{0m}$ are determined at the last step of the solution procedure by solving the coupled problem as will be described in the following sections.

### Eigen-vibrations of the layered medium

A solution to the equations of motion of the soil and the fluid domain which satisfies the boundary conditions at infinity, i.e. Eqs. (20), can be expressed in the following form:

$$\begin{aligned}
\tilde{\varphi}_f(r,z,\omega) &= \mathrm{H}_0^{(2)}(k_f r)\ \left[A_1 \exp(-\alpha_f z) + A_2 \exp(\alpha_f z)\right] \\
\tilde{\varphi}_s(r,z,\omega) &= \mathrm{H}_0^{(2)}(k_L r)\ \left[A_3 \exp(-\alpha_s z) + A_4 \exp(\alpha_s z)\right] \\
\tilde{\psi}_s(r,z,\omega) &= \mathrm{H}_1^{(2)}(k_T r)\ \left[A_5 \exp(-\beta_s z) + A_6 \exp(\beta_s z)\right]
\end{aligned} \tag{25}$$

, with $a_f = \sqrt{k_f^2 - \dfrac{\omega^2}{c_f^2}}$ , $a_s = \sqrt{k_L^2 - \dfrac{\omega^2}{c_L^2}}$ and $\beta_s = \sqrt{k_T^2 - \dfrac{\omega^2}{c_T^2}}$ .

By using the introduced Helmholtz decomposition, the displacements and stresses of the soil domain can be expressed in terms of the potential functions. In a similar way the pressure and velocity field in the fluid can be expressed in terms of the fluid velocity potential. Therefore all physical quantities of the system can be expressed as functions of the corresponding potentials. Substitution of those into Eqs. (14) – (19) yields the following system of coupled algebraic equations:

$$
\begin{aligned}
& -\mathrm{i}\omega\rho_f\left(A_1+A_2\right)\mathrm{H}_0^{(2)}\left(k_f r\right)=0 \\
& -\mathrm{i}\omega\rho_f\left[A_1\exp\left(\alpha_f\left(z_1-z_2\right)\right)+A_2\exp\left(-\alpha_f\left(z_1-z_2\right)\right)\right]\mathrm{H}_0^{(2)}\left(k_f r\right)+ \\
& +\left[-\lambda_s k_L^2 A_3-\lambda_s k_L^2 A_4+2\mu_s\alpha_s^2 A_3+2\mu_s\alpha_s^2 A_4+\lambda_s\alpha_s^2 A_4\right]\mathrm{H}_0^{(2)}\left(k_L r\right)+ \\
& +\left[-2\mu_s k_T^2\beta_s^2 A_5+2\mu_s k_T^2\beta_s^2 A_6\right]\mathrm{H}_0^{(2)}\left(k_T r\right)=0 \\
& 2k_L^2\alpha_s\mu_s\left(A_3-A_4\right)\mathrm{H}_1^{(2)}\left(k_L r\right)-\mu_s\left[k_T^2 A_5+k_T^2 A_6+\beta_S^2 A_5+\beta_S^2 A_6\right]\mathrm{H}_1^{(2)}\left(k_T r\right)=0 \\
& \left[\alpha_f A_1\exp\left(\alpha_f\left(z_1-z_2\right)\right)-\alpha_f A_2\exp\left(-\alpha_f\left(z_1-z_2\right)\right)\right]\mathrm{H}_0^{(2)}\left(k_f r\right)+ \\
& +\mathrm{i}\omega\alpha_s\left(A_4-A_3\right)\mathrm{H}_0^{(2)}\left(k_L r\right)++\mathrm{i}\omega k_T\left(A_5+A_6\right)\mathrm{H}_0^{(2)}\left(k_T r\right)=0 \\
& \left[-\alpha_s A_3\exp\left(-\alpha_s\left(L-z_2\right)\right)+\alpha_s A_4\exp\left(\alpha_s\left(L-z_2\right)\right)\right]\mathrm{H}_0^{(2)}\left(k_L r\right)+ \\
& +\left[-k_T A_5\exp\left(-\beta_s\left(L-z_2\right)\right)+k_T A_6\exp\left(\beta_s\left(L-z_2\right)\right)\right]\mathrm{H}_0^{(2)}\left(k_T r\right)=0 \\
& \left[-k_L A_3\exp\left(-\alpha_s\left(L-z_2\right)\right)-k_L A_4\exp\left(\alpha_s\left(L-z_2\right)\right)\right]\mathrm{H}_1^{(2)}\left(k_L r\right)+ \\
& +\left[\beta_s A_5\exp\left(-\beta_s\left(L-z_2\right)\right)-\beta_s A_6\exp\left(\beta_s\left(L-z_2\right)\right)\right]\mathrm{H}_1^{(2)}\left(k_T r\right)=0
\end{aligned}
\tag{26}
$$

The aforementioned system can be satisfied at all ranges $r$ if and only if:

$$k_L=k_T=k_f=k_r \tag{27}$$

Substitution of this expression into the equations above yields:

$$\mathbf{Da}=\mathbf{0} \tag{28}$$

For a non-trivial solution $\det(\mathbf{D})$ should be set equal to zero, which results in a set of discrete real and imaginary wavenumbers $k_p$, $p=1,2,3,...,\infty$ for each excitation frequency. Each wavenumber corresponds to a mode (the so-called eigenfunction) so that the final response can be represented as a modal sum over all eigenmodes:

$$
\begin{aligned}
\tilde{\varphi}_f(r,z,\omega) &= \sum_{p=1}^{\infty}\mathrm{C_p}\mathrm{H}_0^{(2)}\left(k_p r\right)\tilde{\varphi}_{f,p}(z) \\
\tilde{\varphi}_s(r,z,\omega) &= \sum_{p=1}^{\infty}\mathrm{C_p}\mathrm{H}_0^{(2)}\left(k_p r\right)\tilde{\varphi}_{s,p}(z) \\
\tilde{\psi}_s(r,z,\omega) &= \sum_{p=1}^{\infty}\mathrm{C_p}\mathrm{H}_1^{(2)}\left(k_p r\right)\tilde{\psi}_{s,p}(z)
\end{aligned}
\tag{29}
$$

All other physical quantities can be expressed in terms of the aforementioned potentials, i.e. for the displacement vector of the soil we can write down:

$$
\tilde{\mathbf{u}}(r,z,\omega)=\left\{
\begin{aligned}
\tilde{u}_{r,s}(r,z,\omega) &= \sum_{p=1}^{\infty}\mathrm{C_p}\mathrm{H}_1^{(2)}\left(k_p r\right)\tilde{u}_{r,s,p}(z) \\
\tilde{u}_{z,s}(r,z,\omega) &= \sum_{p=1}^{\infty}\mathrm{C_p}\mathrm{H}_0^{(2)}\left(k_p r\right)\tilde{u}_{z,s,p}(z)
\end{aligned}
\right\}\text{ etc.}
\tag{30}
$$

**Orthogonality relations and correlation of the modal coefficients**

An appropriate integral representation of the interface conditions (21) - (23) correlates the unknown modal coefficients of the shell structure $A_{nm}$ with those of the soil-fluid domain $C_p$. The linear combination can be found by using the orthogonality relation of the fluid-soil modes. The orthogonal domain of the shell structure *in vacuo* is the domain $0\le z\le L$.

Accordingly, the orthogonal domain of the combined fluid-soil modes is the domain $z_1 \le z \le L$. In mathematical terms the orthogonality property for the shell modes implies that:

$$\int_0^L \mathbf{u}_{0m}\mathbf{u}_{0k}dz = N_{0m}\delta_{mk} \tag{31}$$

, where $\mathbf{u}_{0m}$ and $\mathbf{u}_{0k}$ refer to two different shell modes. The norm $N_{0m}$ becomes:

$$N_{0m} = \int_0^L U_{z0m}^2 + U_{r0m}^2 dz \tag{32}$$

Based on integral representation theorems of elastodynamics and a derivation similar to that followed by *Herrera* (Herrera, 1964), it can be shown that for the case of a layered medium occupying the domain $z_1 \le z \le L$, the following orthogonality condition holds:

$$\int_{z_1}^L \left[ \zeta_{s;f} k_q^2 \frac{\tilde{u}_{r,p}(z)}{k_p}\frac{\tilde{u}_{r,q}(z)}{k_q} + \eta_{s;f}\frac{\tilde{u}_{r,p}(z)}{k_p}\tilde{\sigma}_{zz,q}(z) + \tilde{u}_{z,q}(z)\frac{\tilde{\sigma}_{zr,p}(z)}{k_p}\right] dz = \Gamma_p\delta_{pq} \tag{33}$$

, in which $\zeta_{s;f}$ and $\eta_{s;f}$ are given by:

$\zeta_s = \dfrac{\rho_s\left[c_L^4 - \left(c_L^2 - 2c_T^2\right)^2\right]}{c_L^2}$, $\zeta_f = 0$, $\eta_s = \dfrac{c_L^2 - 2c_T^2}{c_L^2}$ and $\eta_f = 1$. Note also that for the fluid zone $\tilde{\sigma}_{zz,q}(z) = -p_{f,q}(z)$. The soil-fluid modes can be normalized such that:

$$\Gamma_p = \int_{z_1}^L \left[ \zeta_{s;f} k_p^2 \tilde{u}_{r,p}^2(z) + \eta_{s;f}\frac{\tilde{u}_{r,p}(z)}{k_p}\tilde{\sigma}_{zz,p}(z) + \tilde{u}_{z,p}(z)\frac{\tilde{\sigma}_{zr,p}(z)}{k_p}\right] dz = 1 \tag{34}$$

We first expand the interface conditions at $r = R$, i.e. (21) – (23) in the modal-wavenumber domain, i.e. in terms of Eqs.(30). By pre-multiplying both sides of each equation with appropriate stress or displacement functions and after carrying out an integration over the soil-fluid domain we obtain the following system of algebraic equations correlating the unknown shell and soil-fluid coefficients:

$$\sum_{m=1}^{\infty} A_{0m}\ Q_{mp} = C_p k_p \mathrm{H}_1^{(2)}\left(k_p R\right)\Gamma_p + \sum_{q=1}^{\infty} C_q L_{qp}\ , \tag{35}$$

with:

$$Q_{mp} = \int_{z_1}^L \left[ \zeta_{s;f} k_p U_{r0m}(z)\tilde{u}_{r,p}(z) + \eta_{s;f} U_{r0m}(z)\tilde{\sigma}_{zz,p}(z) + U_{z0m}(z)\frac{\tilde{\sigma}_{zr,p}(z)}{k_p}\right] dz$$

$$L_{qp} = \mathrm{H}_1^{(2)}\left(k_q R\right)\int_{z_2}^L \left[\tilde{u}_{z,p}(z)\tilde{\sigma}_{zr,q}(z)\right] dz - \mathrm{H}_0^{(2)}\left(k_q R\right)\int_{z_2}^L \left[\tilde{u}_{z,q}(z)\frac{\tilde{\sigma}_{zr,q}(z)}{k_q}\right] dz$$

**Solution to the coupled problem**

A substitution of the modal representation of the two sub-systems into Eq. (10) yields:

$$\begin{gathered}\sum_{m=0}^{\infty}\{\mathbf{L}\}\ A_{0m}\tilde{\mathbf{U}}_{0m}(z) + \left\{\tilde{\mathbf{I}}_{\mathbf{mod}}\right\}\ A_{0m}\tilde{\mathbf{U}}_{0m}(z) = \\ = -H(z - z_2)\cdot\sum_{p=1}^{\infty} C_p\tilde{\boldsymbol{\sigma}}_{s,p}(R,z) + \left[H(z - z_1) - H(z - z_2)\right]\cdot\sum_{p=1}^{\infty} C_p\tilde{\mathbf{p}}_{f,p}(R,z) + \tilde{\mathbf{f}}_{ext}(z)\cdot\delta(z)\end{gathered} \tag{36}$$

By applying the orthogonality property of the shell modes, the following set of coupled algebraic expressions can be obtained:

$$A_{0m}\cdot I_{0m}=-\sum_{p=0}^{\infty}C_p\left[\int_{z_2}^{L}\tilde{\mathbf{U}}_{0m}(z)\cdot\tilde{\boldsymbol{\sigma}}_{s,p}(R,z)+\int_{z_1}^{z_2}\tilde{\mathbf{U}}_{0m}(z)\cdot\tilde{\mathbf{p}}_{f,p}(R,z)\right]dz+\int_{0}^{L}\tilde{\mathbf{f}}_{ext}(z)\cdot\delta(z)\ dz \tag{37}$$

Eqs. (35) and (37) form a coupled system of algebraic equations which need to be solved simultaneously for both $A_{0m}$ and $C_p$ for an externally applied force at the pile head.

## WAVENUMBER INTEGRATIONS METHODS VERSUS MODAL ANALYSIS

In this section the same problem is solved with the use of the Hankel transform method (HTM) with respect to the radial coordinate of the system. This allows us to prove the validity of Eq.(27) and to discuss some of the main similarities and differences between the separation of variables method (SVM) and the HTM. The unified treatment discussed here shows that the modal method is nothing more but a special case of the more powerful integral transform technique. Therefore one should always be aware of the simplifications introduced by the SVM and of the fact that the completeness of the modal sum is not *a priori* guaranteed.

### Solution based on the Hankel transform method

Eq. (28) can actually be obtained by searching for all the potentials in the form of the inverse Hankel transform defined at the interval $r\geq R$:

$$f(r)=\int_0^{\infty}\xi\ F^{H_n}(\xi)\ \mathrm{J}_n(\xi r)d\xi \tag{38}$$

Using the above representation, Eqs.(11)-(13) can be transformed to:

$$\frac{d^2\hat{\varphi}_f^{H_0}(\xi,z,\omega)}{dz^2}-\alpha_f^2\hat{\varphi}_f^{H_0}(\xi,z,\omega)=0,\ \text{with}\quad a_f^2=\xi^2-\frac{\omega^2}{c_f^2} \tag{39}$$

$$\frac{d^2\hat{\varphi}_s^{H_0}(\xi,z,\omega)}{dz^2}-\alpha_s^2\hat{\varphi}_s^{H_0}(\xi,z,\omega)=0,\ \text{with}\quad a_s^2=\xi^2-\frac{\omega^2}{c_L^2} \tag{40}$$

$$\frac{d^2\hat{\psi}_s^{H_1}(\xi,z,\omega)}{dz^2}-\beta_s^2\hat{\psi}_s^{H_1}(\xi,z,\omega)=0,\ \text{with}\quad \beta_s^2=\xi^2-\frac{\omega^2}{c_T^2} \tag{41}$$

The solutions to the above equations are given by:

$$\begin{aligned}
\hat{\varphi}_f^{H_0}(\xi,z,\omega)&=A_1\exp(-\alpha_f z)+A_2\exp(\alpha_f z)\\
\hat{\varphi}_s^{H_0}(\xi,z,\omega)&=A_3\exp(-\alpha_s z)+A_4\exp(\alpha_s z)\\
\hat{\psi}_s^{H_1}(\xi,z,\omega)&=A_5\exp(-\beta_s z)+A_6\exp(\beta_s z)
\end{aligned} \tag{42}$$

The pressures, stresses and displacements of the two media are given by:

$$\begin{aligned}
\tilde{p}(r,z,\omega)&=-\mathrm{i}\omega\rho_f\int_0^{\infty}\xi\ \hat{\varphi}_f^{H_0}(\xi,z,\omega)\ \mathrm{J}_0(\xi r)d\xi\\
\tilde{v}_{z,f}(r,z,\omega)&=\int_0^{\infty}\xi\ \frac{d\hat{\varphi}_f^{H_0}(\xi,z,\omega)}{dz}\ \mathrm{J}_0(\xi r)d\xi\\
\tilde{u}_{r,s}(r,z,\omega)&=-\int_0^{\infty}\xi\left[\frac{d\hat{\psi}_s^{H_1}(\xi,z,\omega)}{dz}+\xi\hat{\varphi}_s^{H_0}(\xi,z,\omega)\right]\mathrm{J}_1(\xi r)d\xi
\end{aligned} \tag{43}$$

$$\tilde{u}_{z,s}(r,z,\omega)=\int_0^\infty \xi \left[\frac{d\hat{\varphi}_s^{H_0}(\xi,z,\omega)}{dz}+\xi\hat{\psi}_s^{H_1}(\xi,z,\omega)\right] \mathrm{J}_0(\xi r)d\xi$$

$$\tilde{\sigma}_{zz,s}(r,z,\omega)=\int_0^\infty \xi \left[-\lambda_s\xi^2\hat{\varphi}_s^{H_0}(\xi,z,\omega)+(\lambda_s+2\mu_s)\frac{d^2\hat{\varphi}_s^{H_0}(\xi,z,\omega)}{dz^2}+2\mu_s\xi\frac{d\hat{\psi}_s^{H_1}(\xi,z,\omega)}{dz}\right] \mathrm{J}_0(\xi r)d\xi$$

$$\tilde{\sigma}_{zr,s}(r,z,\omega)=-\mu_s\int_0^\infty \xi \left[2\xi\frac{d\hat{\varphi}_s^{H_0}(\xi,z,\omega)}{dz}+\frac{d^2\hat{\psi}_s^{H_1}(\xi,z,\omega)}{dz^2}+\xi^2\hat{\psi}_s^{H_1}(\xi,z,\omega)\right] \mathrm{J}_1(\xi r)d\xi$$

A substitution of these solutions into the boundary and interface conditions, i.e. Eqs. (14)-(19), yields the system of equations (28) with the following equivalence $\xi = k_r$. Since the boundary conditions have to be satisfied for all $r \geq R$, it is clear that they must be satisfied by the kernels in the integral representations resulting from substitution of Eqs.(43) into the boundary conditions. This statement is equivalent to the one introduced earlier by Eq.(27). In other words, by setting the separation constants equal to each other we actually make sure that the modes will satisfy the boundary conditions at every $r$. The analogy between the SVM and the HTM in this particular problem actually proves the validity of Eq.(27).

**Case of a bounded domain in depth**

The derivation presented in the previous section clearly demonstrates the close relationship between the wavenumber integration methods and modal analysis methods. However, the modal representation is exact only when the modal sum is complete, which actually implies that additional wavenumbers, other than those located by solving the soil-fluid eigenproblem, do not contribute to the field. To illustrate this, we first note that the Bessel functions of the first kind introduced in Eqs. (43) can be replaced by $\frac{1}{2}\mathrm{H}_n^{(2)}(\xi r)$ with the simultaneous extension of the lower integration limit to $\xi \to -\infty$. The resulting integrals can be evaluated using the contour integration approach and the residue theorem. It is important to note here that the kernels of the inverse Hankel transforms are single-valued functions of $\xi$ despite of the existence of the square roots $a_{f;s} = \sqrt{\xi^2 - \frac{\omega^2}{c_{f;L}^2}}$ and $\beta_s = \sqrt{\xi^2 - \frac{\omega^2}{c_T^2}}$ in the integrands. This can be easily verified by checking the invariance of the integrands with respect to the substitution $\xi = -\xi$. Given the single-valuedness of the integrands, in the evaluation of the integrals by means of the contour integration method, only the poles need to be accounted for. One can locate the poles in the complex plane by simply solving Eq.(28). Positions of the poles are shown indicatively in Fig. 2. The physical meaning of the real and imaginary poles which represent the radial wavenumbers will be given in the next section. By using Cauchy's theorem the original integration path can be deformed along the real axis to the one depicted by the bolt (blue) line as shown in Fig. 2 into the complex plane in order to avoid the poles. The radiation condition at infinity determines whether the contour should pass below or above the poles on the real axis. The contour integration technique yields the following relation:

$$\int_{-\infty}^{+\infty} + \int_{C-\infty} = 2\pi \mathrm{i}\sum_{\mathrm{p}=1}^{\infty}\mathrm{res}(k_p) \qquad (44)$$

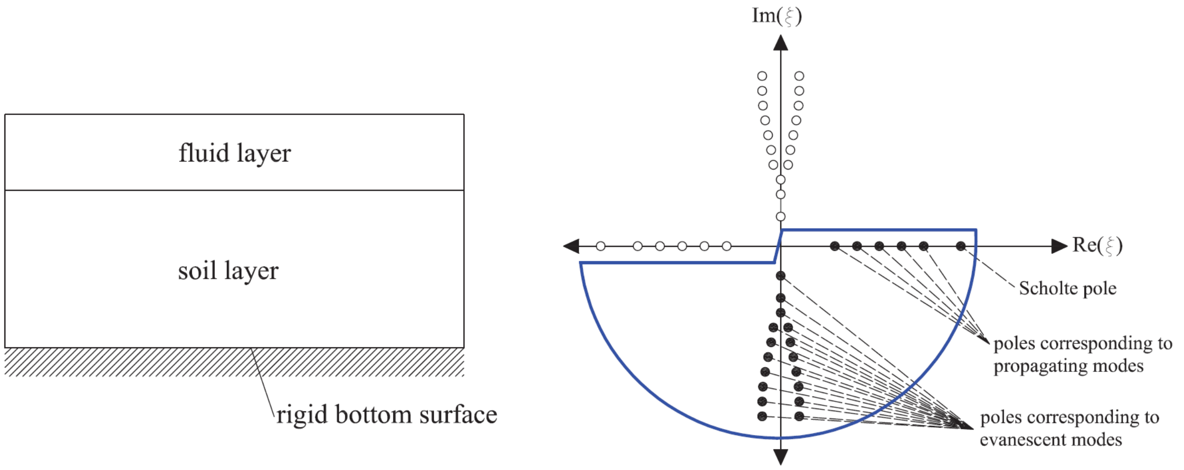


Fig.2 Complex contour integration path for the case of a bounded medium

In Eq.(44) the functions to be integrated are those defined by Eqs.(43). We note that the semicircle $C_{-\infty}$ goes to infinity and subsequently the second integral in (44) goes to zero because the Hankel function decays as the radius of the semicircle increases. Eq.(44) can be rewritten as:

$$\int_{-\infty}^{+\infty} = 2\pi \mathrm{i} \sum_{\mathrm{p}=1}^{\infty} \mathrm{res}\left(k_p\right) \tag{45}$$

, which actually implies that the original integration over the whole range of wavenumbers is equal to the sum of the residues enclosed by the chosen integration path. The residues themselves correspond to the modes of the problem at hand. In other words, the representation of the response of the bounded fluid-soil domain in the form of a modal sum is exact.

**Case of an unbounded domain in depth**

Now let us assume that the soil is not terminated at $z = L$ and that the rigid boundary is replaced by a half-space extending to $z \to +\infty$ (Fig. 3). In this case the integrands are no longer single-valued. Therefore, the appropriate branch cuts should be introduced in the complex $\xi$ – plane as shown in Fig. 3.

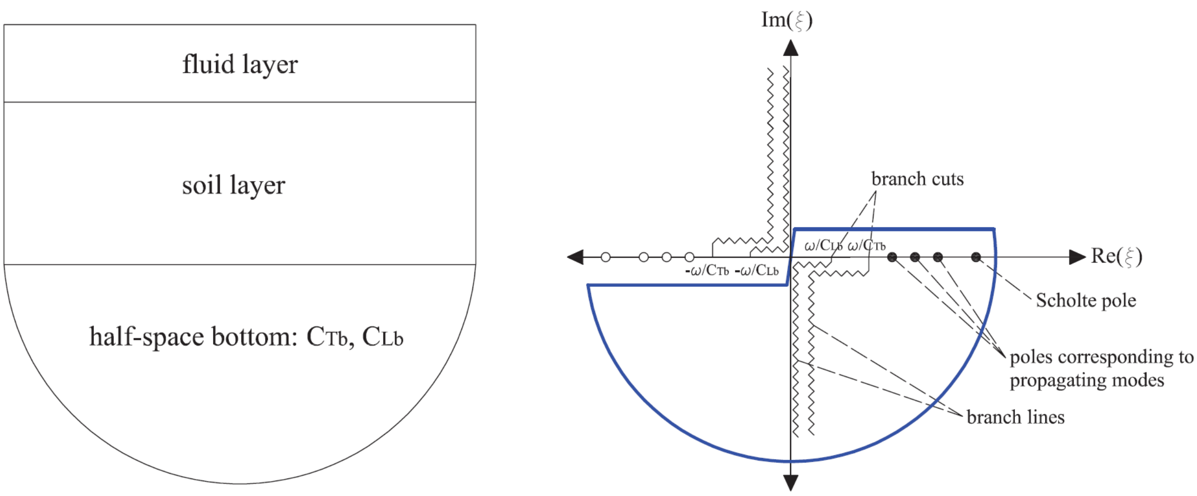


Fig.3 Complex contour integration path for the case of an unbounded medium

Accounting for the integration along the branch cuts, the Cauchy's theorem yields:

$$\int_{-\infty}^{+\infty} + \int_{C-\infty} + \int_{branch} = 2\pi \mathrm{i} \sum_{\mathrm{p}=1}^{\infty} \mathrm{res}(k_p) \tag{46}$$

A comparison of (44) and (46) shows that an additional integral is present over the branch cuts in the case of the half space. In contrast to the bounded domain, this integral will contribute to the resulting deformation field:

$$\int_{-\infty}^{+\infty} = 2\pi \mathrm{i} \sum_{\mathrm{p}=1}^{\infty} \mathrm{res}(k_p) - \int_{branch} \tag{47}$$

The additional contribution of the branch line integrals clearly makes the modal sum incomplete. A physical interpretation of this result is as follows. The branch cuts contributing to the above equation in terms of leaky waves correspond to $0 < \xi < \omega / c_{Lb;Tb}$. By understanding the fact that the Hankel representation is actually a decomposition of the field in terms of conical waves, the small wavenumbers $\xi \le \left| \omega / c_{Lb;Tb} \right|$, will correspond to steep angles of incidence of the conical fronts on the half space surface ($z = L$). For those steep angles of incidence radiation of energy in the form of body waves in the half space is unavoidable. This continuous radiation is not captured by the normal modes which actually represent only that part of the spectrum corresponding to the energy trapped in the waveguide. The simplification originally introduced by the rigid bottom hypothesis at $z = L$ becomes now apparent. In this latter case, even wave fronts with steep angles of incidence do not lose any energy when reflecting from the bottom of the system and the energy is *locked* in the waveguide which, in turn, makes Eq.(45) valid. In this work we would like to interpret this result from a different point of view. By checking whether the generated wave fronts from the pile vibrations in the soil zone are formed with large or small angles to the vertical we can directly conclude as to whether the modal summation is a good representation of reality or not. As will be shown later, for large penetration depths of the pile into the soil, the main part of the energy will indeed be trapped in the waveguide which makes our representation of the response in the form of Eq.(45) valid for almost all cases of practical interest.

## NUMERICAL RESULTS

In this section the response of the coupled system is examined for a specific set of material and geometrical parameters similar to those introduced in (A.Tsouvalas and A.V.Metrikine, 2013).

| Parameter | Value | Units | Parameter | Value | Units |
|---|---|---|---|---|---|
| E | 2,10E+11 | N/m$^2$ | $v_s$ | 0,40 | - |
| v | 0,28 | - | $\rho_s$ | 1600 | Kg/m$^3$ |
| $\rho$ | 7850 | Kg/m$^3$ | $E_s$ | 1,00E+08 | N/m$^2$ |
| $\eta_{shell}$ | 0,001 | - | $G_s$ | 3,57E+07 | N/m$^2$ |
| R | 0,46 | m | $\lambda_s$ | 1,43E+08 | N/m$^2$ |
| 2h | 0,02 | m | $c_L$ | 366 | m/s |
| L | 32,4 | m | $c_T$ | 149 | m/s |
| z1 | 6,50 | m | $\rho_f$ | 1000 | Kg/m$^3$ |
| z2 | 13,4 | m | $c_f$ | 1500 | m/s |

Table 1. Material constants, geometrical parameters and soil properties (reference values) for the examined case

The geometrical configuration and material properties are those given in table 1 unless stated otherwise. At first, the dispersion relation of the exterior (to the pile) domain is examined since this is essential in order to understand and analyse the various types of waves that can propagate in the media. Secondly, the forced response of the system is examined in both time and frequency domains. Finally, the soil parameters are modified in order to check the sensitivity of the response for different soil properties. Special attention is paid to the examination of the influence of the Scholte waves on the pressure levels in fluid.

## Dispersion relation and waveforms

The obtained dispersion relation ($\omega - k_p$ diagram) for the propagating modes of the exterior soil-fluid domain is shown in Fig.4. The term propagating modes is used here to reflect modes with purely real wavenumbers in the case of a perfectly elastic solid or complex wavenumbers with a real part being much larger than the imaginary one for those cases in which material dissipation is included. Each point on the graph represents a solution of the dispersion relation of the exterior domain. The three phase velocities are easily distinguishable and are marked with thick bold lines for comparison. In the dispersion plot, the distinguished root resulting in the lowest phase velocity corresponds to the Scholte wave travelling along the seabed interface. This root is present for any soil-fluid configuration. On the contrary, the leaky-Rayleigh wave becomes forbidden for most cases of practical interest because the phase velocity of the shear waves in the soil medium is much smaller than that of the bulk waves in the fluid. The Scholte wave corresponds to a purely real wavenumber in a perfectly elastic solid. Its amplitude decays exponentially as one moves away from the interface in both media and as such it is a true interface wave. A detailed description of the aforementioned waveforms can be found elsewhere (Glorieux et al., 2001).

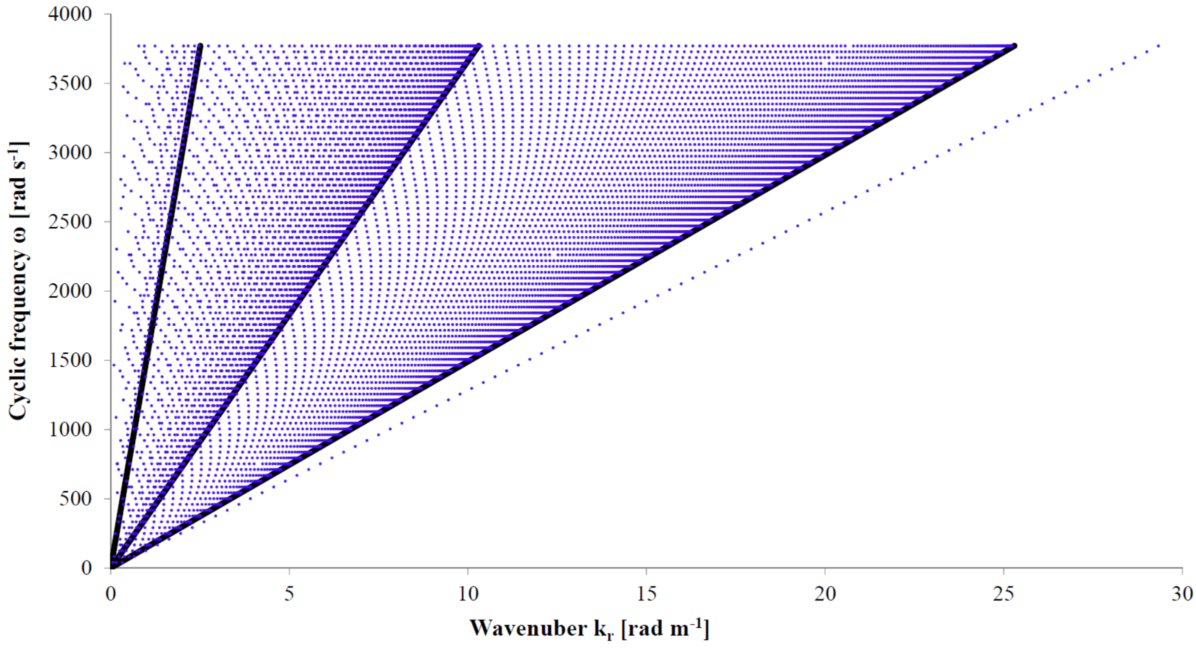


Fig.4 Dispersion relation for frequencies up to 600Hz (propagating modes only)

**Forced response of the system**

In this section, results are presented for the case of a system with the geometrical configuration and the material properties as given in table 1. The load is applied at the pile head with no inclination to the vertical. The external load corresponds to a hammer input energy of 90 kJ. The maximum force amplitude equals 12 MN and the duration of the main pulse is equal to 5 ms.

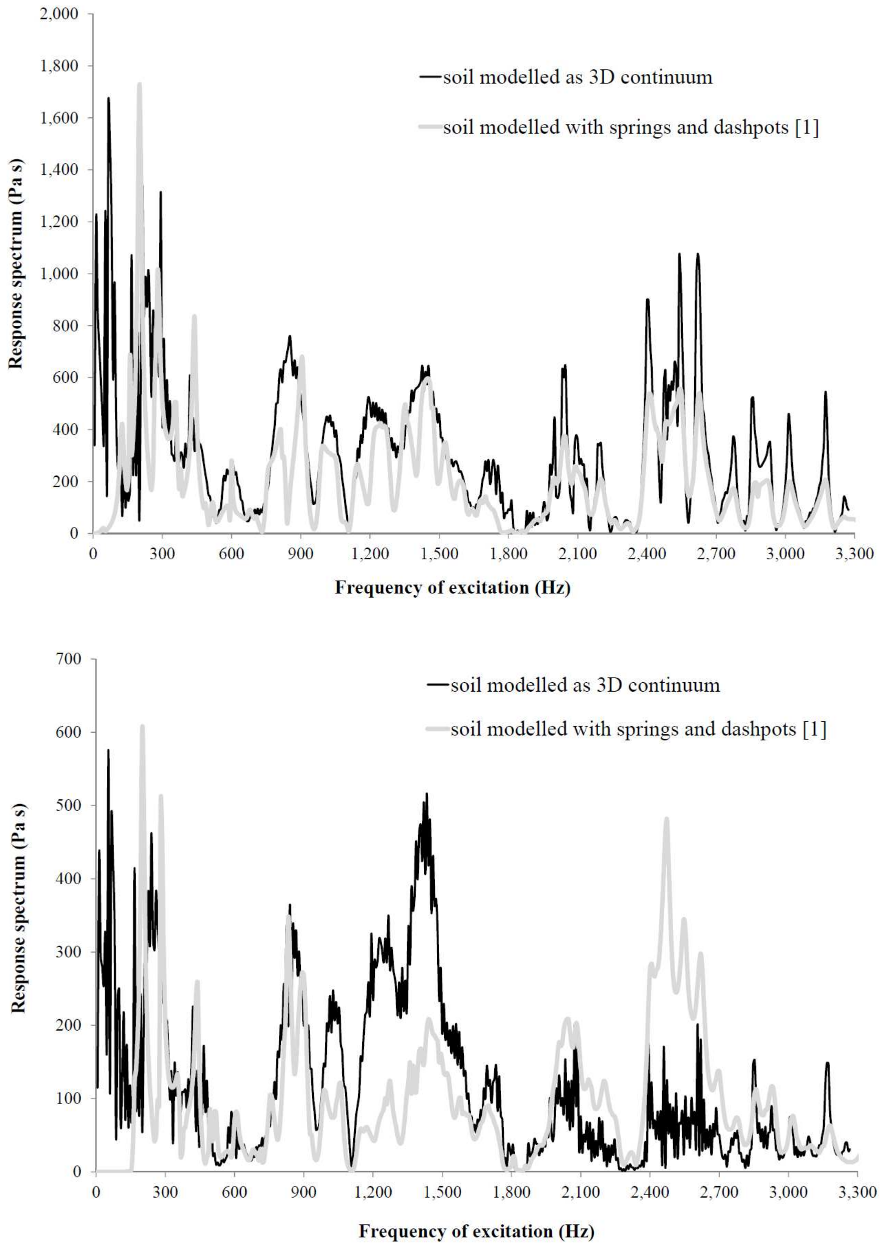


(a)

(b)

Fig.5 Pressure amplitude spectra of the fluid in Pa s for (a) r=1 m and (b) r=15 m from the surface of the pile and for a depth equal to 5.5 m from the sea surface

In Fig.5 pressure amplitude spectra are shown for two radial distances and for a point positioned close to the seabed surface. The pressure amplitudes are plotted versus the ones obtained using a similar model developed in (A.Tsouvalas, A.V.Metrikine, 2013), in which the soil is described by distributed spring and dashpots. As can be seen, the results are similar for frequencies higher than 500 Hz. For lower frequencies, the difference in the pressure amplitudes between the two models is large. The sharp cut-off frequency present in the case of (A.Tsouvalas, A.V.Metrikine, 2013) disappears when a three-dimensional description of the soil is included. The soil seems to play a major role in the lower frequency regime where the coupling between the soil vibrations and the fluid zone is strong.

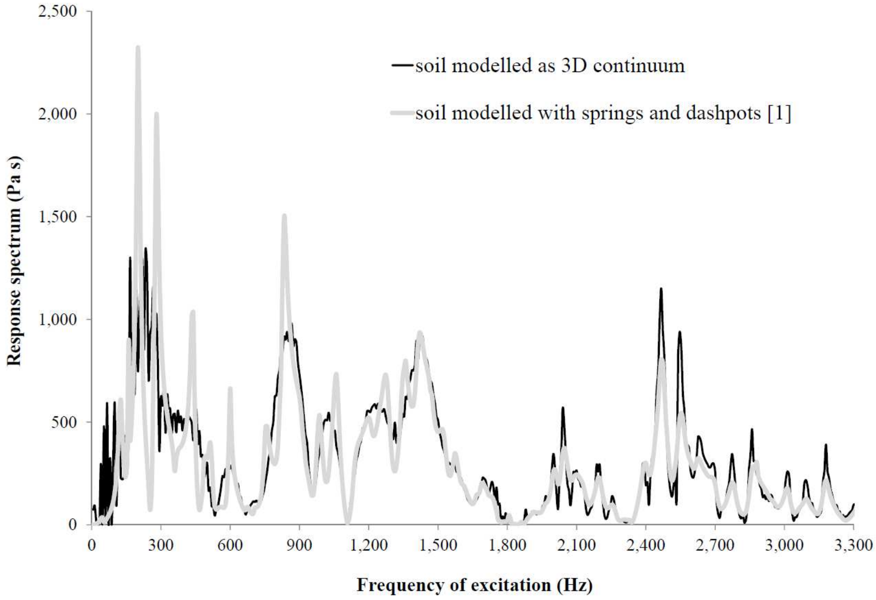


(a)

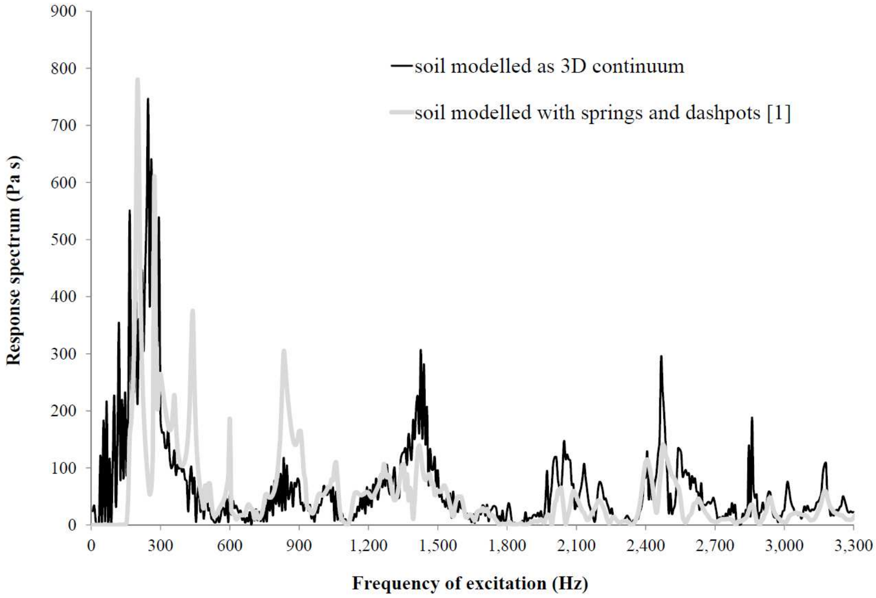


(b)

Fig.6 Pressure amplitude spectra of the fluid in Pa s for (a) r=1 m and (b) r=15 m from the surface of the pile and for a depth equal to 2 m from the sea surface

In Fig.6 results are presented for a point positioned 2m from the sea surface. Here the differences in the lower frequencies are smaller because of the fact that the sea surface is assumed to be free in both models. In Fig.7, displacement amplitude spectra of the soil are shown for a point positioned on the seabed and for two radial distances. It can be noticed that the soil contributes significantly to the field at frequencies lower than 400 Hz.

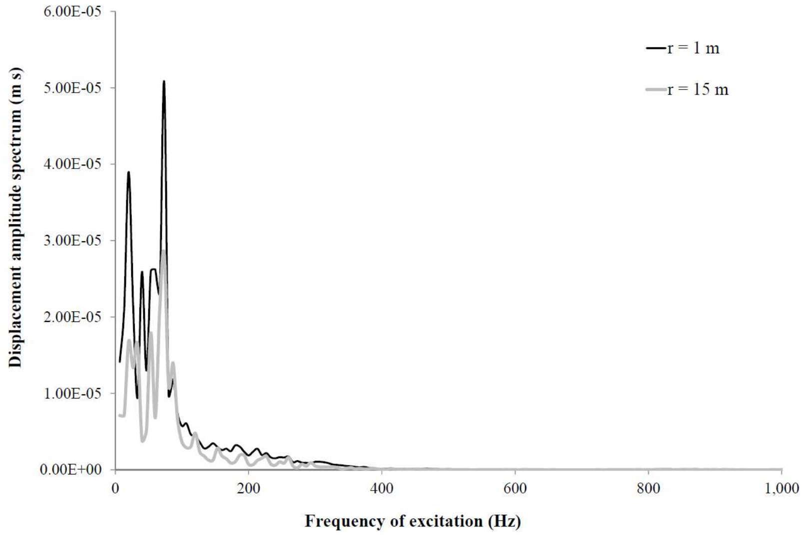


Fig.7 Displacement amplitude spectra for the soil in m s for r=1 m and r=15 m from the surface of the pile and for a point positioned at the seabed surface

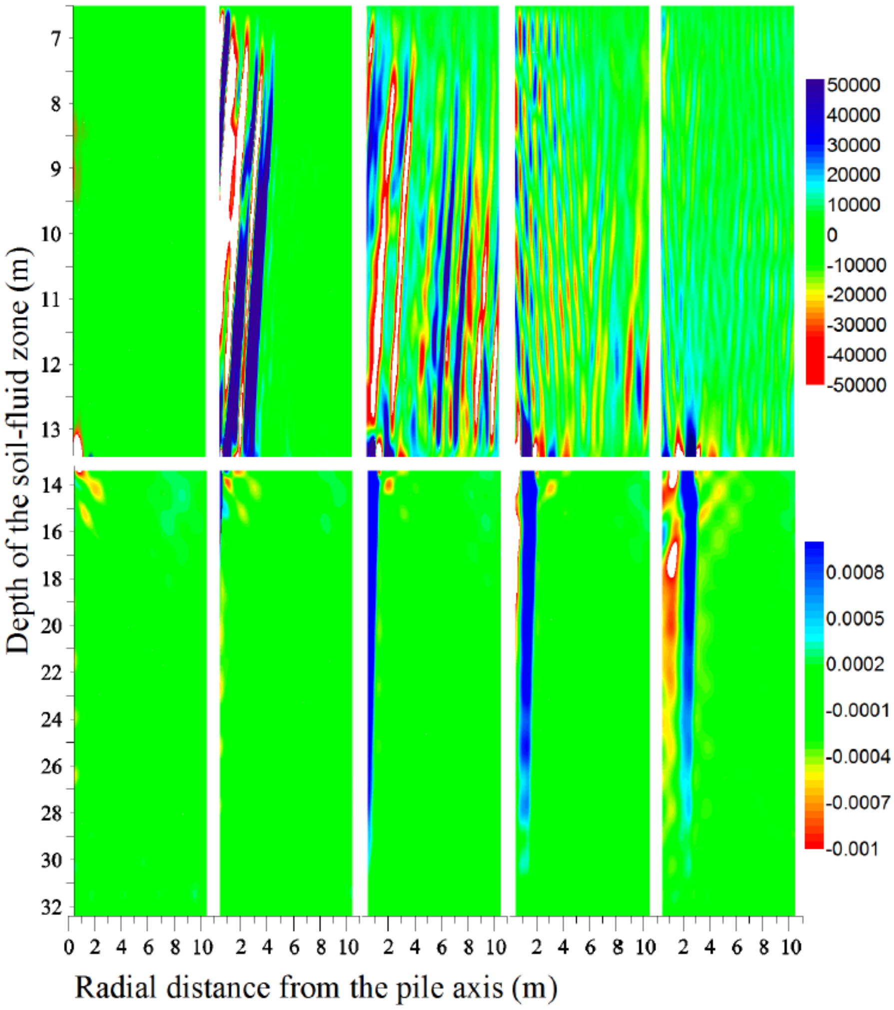


Fig.8 Pressures in the fluid (top) and vertical displacements in the soil (bottom) for different time moments after the impact (from left to right: t=1ms; t=5ms; t=10ms; t=15ms; t=25ms)

In Fig.8 the generated wave field is shown. The near-field response in the fluid zone is dominated by pressure Mach cones due to the supersonic compressional waves in the pile generated by the impact hammer. These waves are formed with an angle of approximately $\sin^{-1}(c_f / c_p) = \sin^{-1}(1500/5000) = 17^0$ to the vertical. The soil response is dominated by shear waves with almost vertical polarization. In this particular example the inclination of the shear fronts to the vertical is less than $2^0$. Scholte waves are generated at the seabed interface and propagate with a velocity slightly lower than that of the shear waves in the soil as can be seen from the slight bending of the shear fronts close to the seabed interface. In this example the estimated Scholte wave speed is approximately equal to $0.89c_T = 133\,\mathrm{ms}^{-1}$.

Finally, in Fig.9 the generated velocity pulse propagating downward the pile is shown. The horizontal axis shows the vertical velocity in $\mathrm{ms}^{-1}$ and the vertical axis shows the distance from the pile head. As can be seen the wavefront propagates with a velocity slightly higher than 5000 $\mathrm{ms}^{-1}$. It is worth to mention that the region in front of the first wavefront remains quiescent until the first wave reaches it. The sharpness of the front for the frequencies involved is guaranteed by the high order thin shell theory applied in this case which includes high order effects like shear deformation and rotational inertia.

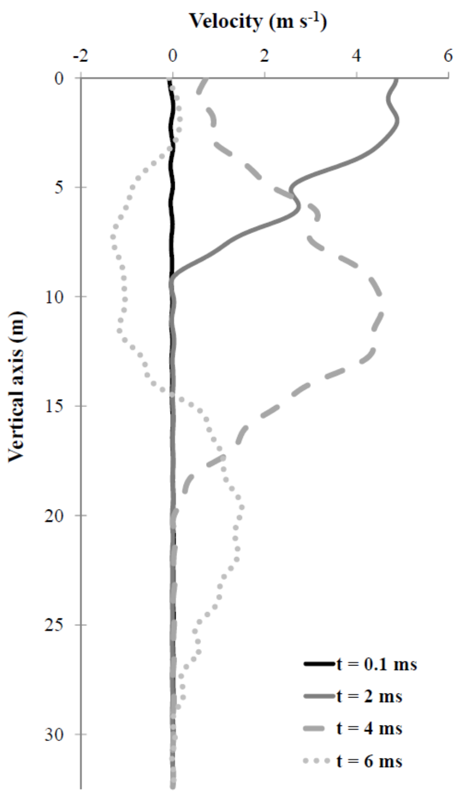


Fig.9 Velocity evolution with time for the shell structure

## Influence of the soil elasticity

In this section, the soil stiffness $E_s$ is varied in order to examine its influence on the response of the coupled system. Three cases are examined which are summarised in table 2. The rest of the material properties are kept constant and are given in table 1.

| Parameter | Value | Units | Parameter | Value | Units | Parameter | Value | Units |
|---|---|---|---|---|---|---|---|---|
| $E_1$ | 1,00E+8 | N/m$^2$ | $c_{L1}$ | 366 | m/s | $c_{T1}$ | 149 | m/s |
| $E_2$ | 5,00E+8 | N/m$^2$ | $c_{L2}$ | 818 | m/s | $c_{T2}$ | 334 | m/s |
| $E_3$ | 5,00E+7 | N/m$^2$ | $c_{L3}$ | 258 | m/s | $c_{T3}$ | 105 | m/s |

Table 2 Phase velocities for different elasticity moduli

In Fig.10, the pressure amplitude spectra are shown for the three cases and for a point positioned at a depth equal to 5.5m and at a radial distance equal to 5m from the pile surface. The point is again chosen close to the seabed where the influence of the soil is expected to be larger. As can be seen, the differences are significant only at the lower frequency regime, i.e. for $f \leq 400$ Hz. Regarding the response in the time domain the following conclusions can be drawn. Firstly, the pressures in the fluid zone are increased close to the seabed in the case of the stiff soil. Secondly, the stiffer the soil the smaller the penetration depth of the Scholte waves into the soil. For stiffer soils, the energy is mainly localized in the fluid. Similar results have been obtained in other studies regarding the penetration depth of the Scholte waves into solids (Glorieux et al., 2001). The increase of the pressures for stiffer substrates has also a clear physical explanation: stiffer soils provide larger resistance to the compressional waves travelling downwards the pile and therefore most of the energy is reflected upward as soon as from the soil-fluid interface resulting thus in higher pressure levels in the fluid. This phenomenon is less dominant for soft soils in which a larger portion of the input hammer energy is absorbed by the soil in the form of wave radiation. Finally, the shear cones show a larger inclination to the vertical for stiffer soil sediments. For the case in which $E_s = 500$ Mpa, the angle of the shear cones is slightly less than $\sin^{-1}\left(c_T / c_p\right) \approx 4^0$. The shear front bends towards the seabed interface (becomes almost vertical). This strong curvature of the front is mainly attributed to the Scholte wave and is completely absent when the Scholte root is excluded from the modal summation.

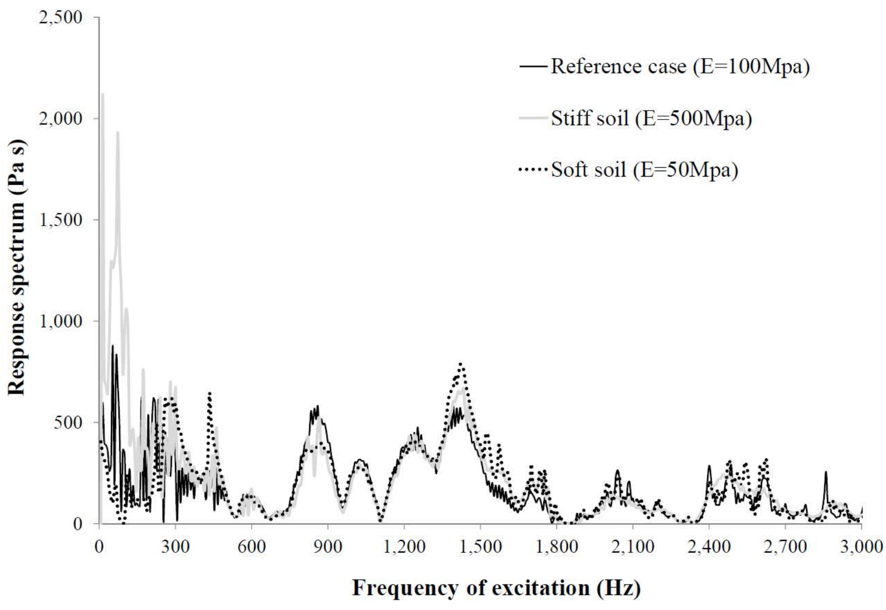


Fig.10 Pressure amplitude spectra of the fluid in Pa s for r=5 m and a depth equal to 5.5 m from the sea surface for different sediment types

## CONCLUSIONS AND DISCUSSION

In this paper a novel approach is presented for the study of the coupled vibro-acoustics of piles in layered media. Although the focus was mainly on the generated pressure field in the fluid column, it is clear that exactly the same model can be used for prediction of vibration levels in the soil region for pile driving activities either offshore on onshore. The pile is described by an appropriate thin shell theory which includes the effects of both shear deformation and rotational inertia. The fluid is modelled as a three-dimensional compressible medium with a pressure release boundary describing the sea surface. The soil is described as a three-dimensional continuum able to support both dilatational and shear waves and is terminated at the pile tip level with a rigid boundary. The influence of the rigid boundary is discussed on the basis of complex contour integrations over the horizontal wavenumbers. A comparison of the modal analysis approach with the wavenumber integration method shows that the former is actually a special case of the latter and as such it can be accurate only when certain conditions are met. Thus, the completeness of the modal sum should always be checked since it is not *a priori* guaranteed. In the case of pile driving it is shown that for most cases of practical interest the model can provide reliable predictions of the sound levels in the fluid and of the vibrations levels in the soil. The accuracy increases the larger the penetration depth of the pile into the soil and the softer the soil sediment.

A reference case for which experimental data are available for comparison is analysed in both time and frequency domains. At first, a physical interpretation of the dispersion relation is given. In the dispersion plot, the distinguished root for the lowest phase velocity corresponds to the Scholte wave travelling along the seabed interface. This root is present for any soil-fluid configuration.

The near-field response in the fluid is dominated by pressure Mach cones due to the supersonic compressional waves in the pile generated by the impact hammer. The results are also compared with those of a similar model in which the soil is described by distributed springs and dashpots and are shown to agree well only for medium-high frequencies. For lower frequencies the spring-dashpot model cannot capture the soil-fluid coupling effects correctly. The soil response is dominated by shear waves with almost vertical polarization. Scholte waves are generated at the seabed interface. These waves propagate with a velocity slightly lower than that of the shear waves in the soil. It is shown that the Scholte wave influences the results at the lower frequency regime and in a confined region close to the seabed. The influence of soil elasticity on the response of the system is analysed. As expected, the shear cones in the soil show a larger inclination to the vertical for stiffer soil sediments. The results also indicate that the pressures in the fluid are increased close to the seabed in the case of a stiffer soil.

## REFERENCES

A. Tsouvalas, A.V. Metrikine. A semi-analytical model for the prediction of underwater noise from offshore pile driving. *Journal of Sound and Vibration*, 2013 (article in press), http://dx.doi.org/10.1016/j.jsv.2013.01.026.

Glorieux et al., 2001. On the character of acoustic waves at the interface between hard and soft solids and liquids. *Journal of Acoustical Society of America*, 110(3), pp. 1299-1306.

Herrera I. On a method to obtain a Green's function for a multi-layered half space. *Bulletin of the Seismological Society of America*, Volume 54, No. 4, pp. 1087-1096, 1964.

H.R. Masoumi, G. Degrande. Numerical modeling of free field vibrations due to pile driving using a dynamic soil-structure interaction formulation. *Journal of Computational and Appied Mathematics*, Volume 215, pp. 503-511, 2008.